ISSN: 1410-8917
Jurnal Kimia Sains & Aplikasi
e-ISSN: 2597-9914

Jurnal Kimia Sains dan Aplikasi 25 (9) (2022): 307–315

Jurnal Kimia Sains dan Aplikasi
Journal of Scientific and Applied Chemistry

Journal homepage: http://ejournal.undip.ac.id/index.php/ksa

Fabrication of Cellulose Nanocrystal (CNCs) Based Biosorbent From Oil Palm Trunks Through Acid Hydrolysis With Sonication Assisted and Adsorption Kinetic Study

Pra Cipta Buana Wahyu Mustika [a], Mega Mustikaningrum [b,*]

[a] Chemical Engineering Department, Faculty of Engineering, Universitas Surabaya, Surabaya 60293, Indonesia
[b] Chemical Engineering Department, Faculty of Engineering, Universitas Muhammadiyah Gresik, Gresik 61121, Indonesia

* Corresponding author: megamustikaningrum@umg.ac.id

https://doi.org/10.14710/jksa.25.9.307-315

Article Info

Article history:

Received: 11th August 2022
Revised: 2nd November 2022
Accepted: 16th November 2022
Online: 23rd December 2022

Keywords:
Cellulose nanocrystals; hydrolysis; sonication; biosorbent; oil palm trunk

Abstract

Developing cellulose nanocrystal (CNCs) preparation techniques is a challenge confronted by many researchers. The advantages of property remain the reason for research to be developed. To deal with this issue, it is essential to conduct research related to process optimization, particularly in the hydrolysis process, which is the primary step in forming CNCs. In this study, the effect of sonication-assisted hydrolysis time was investigated. XRD characterization showed that the CNCs formed where the first group with specific peaks indicated. The crystallinity of CNCs decreased with increasing sonication duration, indicating that sonication-assisted hydrolysis was nonselective. The crystallinity of CNCs obtained for 15, 30, and 45 min was 61.6, 55.0, and 48.4 %, respectively. For sonication duration variations of 15, 30, and 45 min, the hydration diameter of CNCs was nearly identical at 42.35 ± 27.10, 42.99 ± 29.46, and 42.63 ± 29.49 nm, respectively. Similarly, the removal of methylene blue can be achieved using CNCs bio-adsorbent. The results of percent removal of methylene blue under sonication treatment of 15, 30, and 45 min of sonication were 73.34; 73.62; 72.86 %, respectively. The adsorption rate of CNCs follows the pseudo-second-order kinetic model, with the adsorption values under sonication treatment of 15, 30, and 45 min were 0.075 ± 0.008; 0.166 ± 0.013; 0.078 ± 0.005 g mg^{-1} min^{-1}, respectively.

1. Introduction

Cellulose nanocrystals (CNCs) are a derivative product of cellulose, a natural polymer available in abundance. The CNCs are a crystalline part of the cellulose constituent system and are separated from the amorphous region [1, 2]. In addition to CNCs, cellulose nanofibrils (CNFs) can also be produced from cellulose through a top-down process similar to that in the production of CNCs [3, 4]. However, the two products have different characteristics, including shape, diameter, length, crystallinity, tensile strength, and elastic modulus [5, 6]. Meanwhile, the applications of the two products often coincide for nanocomposite materials in various fields, including health, catalysts, water-oil separation, and other advanced materials [7, 8, 9]. Developing a sustainable process and materials is necessary based on these advantages and various applications. Different types of biomass can be used as raw materials for sustainable synthesis. In general, its availability is estimated between 75 and 100 billion tons, with the potential to expand if its management is improved. The potential availability of biomass, particularly in Indonesia, may be demonstrated using materials like rice stalks, bagasse, algae, oil palm trunks, and others [10, 11, 12]. The existence of palm oil in Indonesia has been known for a long time since the production of palm oil is the largest in the world. Thus, the sustainability of these resources is no longer a challenge. Therefore, the management and technology of conversion into valuable products such as CNCs or CNFs still need to be further developed.

In this research, technology development is conducted based on an acid hydrolysis reaction accompanied by sonication. The amorphous regions will be broken down during hydrolysis due to the fragility of the amorphous structures [13]. Thus, nano-sized crystalline cellulose products (CNCs). It is also essential to consider the choice of acid for hydrolysis, given that the yield and characteristics are affected during the process. Mineral acids such as sulfuric acid, hydrochloric acid, phosphoric acid, bromic acid, or a mixture of these acids are commonly used [14]. Sulfuric acid will be utilized particularly in this study as opposed to other acids. Using this type of acid leads to CNCs that are more stable across a wider pH range [15].

Apart from stability, the size distribution and crystallinity of CNCs must also be good. The presence of sonication is expected to help achieve these products. During sonication, the waves produce strong oscillations that form on cavitation. Microscopic phenomena include gas formation, expansion, and impulse due to the absorption of ultrasonic energy in a liquid. The presence of high-energy cavitation bubbles is expected to break the hydrolysis-residual amorphous chains to achieve the desired size and distribution of CNCs. The duration of sonication is the focus of the research. The achievement parameters of this process will include crystal size, size distribution, and simple application of CNCs for methylene blue adsorption.

2. Experimental Section

2.1. Materials

Raw materials (oil palm trunks) were supplied from oil palm plantations in Capari village, Cilacap. Sodium hydroxide (NaOH), sodium chlorite ($NaClO_2$), sulfuric acid (H_2SO_4), acetic standard buffer, and methylene blue powder were purchased from Merck. Deionized (DI) water was made using reverse osmosis technology in the laboratory (5 µsiemens).

2.2. Methods

2.2.1. Preparation of CNCs adsorbent

Before processing, the oil palm trunk in the form of barks was processed with a grinder until it was reduced to a size of 40 mesh to obtain a powder-like shape. Oil palm trunks were prepared through mechanical steps, including (1) drying, (2) grinding, and (3) screening. The mechanical process yielded a product with a size specification of less than 60 mesh, whereas the non-mechanical steps include: (1) alkali pretreatment, (2) bleaching, and (3) hydrolysis. Alkaline pretreatment was performed using 3%$^{(w/v)}$ NaOH for 2 h at 80°C. The exact duration and temperature were selected for bleaching, in which 1.7%$^{(v/v)}$ $NaClO_2$ was added at pH 5.

The sample was then neutralized and hydrolyzed with 50%$^{(v/v)}$ H_2SO_4 at 40°C, pH 4, for 45 min. The decision to employ sulfuric acid at this concentration was made considering that sulfuric acid at higher concentrations will convert cellulose into glucose under certain operating conditions. These conditions are also adapted to the operating conditions in many studies. The results of the hydrolysis were then neutralized and sonicated. The hydrolysis results were centrifuged by adding water to the sample for washing. Centrifugation was performed at 700 rpm for 15 min to remove sulfuric acid in the hydrolysis residue. This process was repeated several times until the pH reached neutral. In this case, the sonication duration was varied for 15, 30, and 45 min. As a research limitation, the ultrasonic frequency was low (37 kHz), and the temperature was controlled at ±45°C. The results from the sonication stage were compacted and dried using a freeze dryer for 2-3 days before being utilized for the adsorption process. The working steps in the CNCs extraction series are shown in Figure 1, whereas the process mechanism is microscopically illustrated in Figure 2.

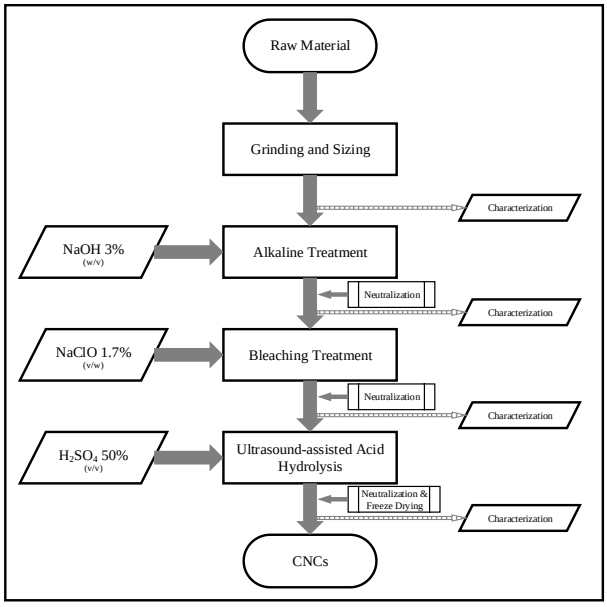

Figure 1. Flow diagram of CNCs extraction from oil palm trunks

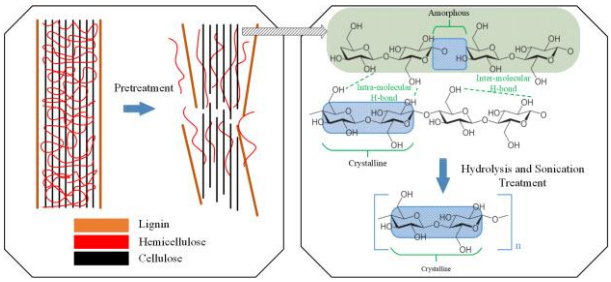

Figure 2. Schematic of CNCs production through acid hydrolysis assisted by sonication

2.2.2. Characterization

The crystallinity of CNCs was investigated using X-ray diffraction (XRD) [Bruker AXS Model D8 Advance Eco], using Cu Kα radiation (λ = 0.154 nm, 40 kV, and 40 mV) and measuring angle (2θ) in the range of 3–90° with a scan rate of 0.4°/min at room temperature. The degree of crystallinity (C[%]) was calculated using the Segal equation (1).

$$C[\%] = \frac{I_{200} - I_{am}}{I_{200}} \times 100\% \quad (1)$$

where, I_{200} is the maximum intensity of the crystalline, otherwise I_{am} refers to the maximum intensity of the

non-crystalline. The peaks of the XRD diffractogram were fitted using a nonlinear curve fit (Gauss) tool in Origin® 2019b. Crystallite size was calculated using the Scherrer formula (2).

$$D_{crystallite} = \frac{0.94\lambda}{\beta_{½}\cos\theta} \quad (2)$$

where θ is the diffraction angle, λ is the X-ray wavelength, and β½ is the full width at half-maximum (FWHM) of the diffraction peak.

Apart from measuring crystallinity and crystal size, the distance between crystal layers can also be calculated using the data obtained from XRD. The calculation was done through equation (3).

$$d_{spacing} = \frac{n\lambda}{2\sin\theta} \quad (3)$$

The hydrodynamic diameter was measured using an particle size analyzer (PSA) [Malvern Nano Z ZEN 2600]. The measurement is based on the Stokes-Einstein equation, which assumes that the particles are spherical in shape and that the interactions formed between the particles-solvent determine the size obtained. The Stoke-Einstein (d_h) equation (4) is written as follows:

$$d_h = \frac{kT}{3\pi\eta D_t} \quad (4)$$

where k, T, η, and D_t are Boltzmann's constant, absolute temperature, colloid viscosity, and diffusivity coefficient, respectively.

2.2.3. Adsorption performance testing on CNCs

The adsorption performance of CNCs as adsorbents was measured for methylene blue. A 300 mL of 1 ppm solution was prepared by dissolving the mass of methylene blue powder in deionized water. CNCs (0.08 g) were added to the prepared solution and then stirred at a low frequency to homogenize the solution. During this process, sampling was done at certain time intervals until it ended at 120 min. Each sampling was duplicated three times at different sample points. Spectrophotometer UV– Vis (Thermo Scientific Model GENESYS™ 30) was used for concentration measurement. Meanwhile, the process occurred at atmospheric pressure and controlled temperature using a water bath (Memmert Model WTB 6) at 30°C. Percent removal that can be achieved from the adsorption process was calculated using equation (5).

$$\text{Removal } [\%] = \frac{C_i - C_e}{C_i} \times 100 \quad (5)$$

where, C_e and C_i are the concentrations at equilibrium and the initial concentrations, respectively.

2.3. Kinetic models

2.3.1. Prediction of the adsorption mechanism

An understanding of the mechanism and kinetic model of an adsorption process is inseparable from the adsorption performance of CNCs itself. The prediction of the methylene blue adsorption mechanism has been proposed by Tan *et al.* [16]. The illustration can be seen in Figure 3.

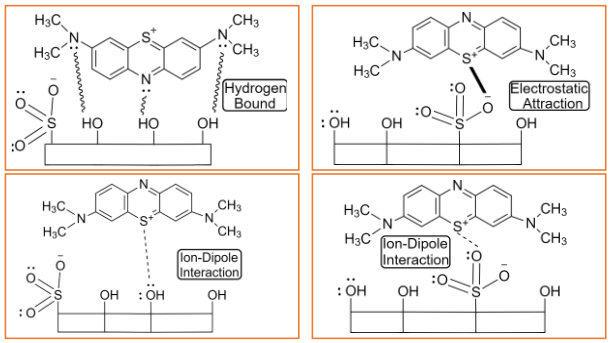

Figure 3. Prediction of the adsorption mechanism that occurs between CNCs and methylene blue [16]

Based on the three predictions of the mechanism, many adsorption kinetics models have been developed, including the Elovich model, Lagergren's first-order model, and the intraparticle diffusion model. These three models will be evaluated and compared with the model developed in this research.

2.3.2. Fundamentals of adsorption kinetics

As is well known, the adsorption kinetics model has been extensively studied. These studies are usually based on assumptions and theoretical approaches to predict the adsorption mechanism. However, research often does not consider this in the selection of models. Therefore, the reasons for taking the three kinetic models will be discussed in this section. Elovich's kinetic model is developed to study the adsorption behavior of gases on heterogeneous solid surfaces. However, as research continues, and many publications have stated that this model can also be used for the adsorption of various contaminants dissolved in liquids. The Elovich model can determine the phenomenon of Cr (VI) adsorption with the adsorbent in biomass waste form [17]. The research report showed the same for As(III) adsorption with manganese ferrite nanoparticles as adsorbent [18]. Research on the adsorption of dye contaminants has also been studied, confirming that the Elovich model can be used to understand the adsorption kinetics [19, 20]. Briefly, Elovich's kinetic model is expressed as equation (6).

$$\frac{dq_t}{dt} = a\exp(-bq_t) \quad (6)$$

where, a (mg.g^{-1}.min^{-1}) is the rate of adsorption at the start of the process, b (g.mg^{-1}) is the Elovich constant, and q_t (mg.g^{-1}) is amount adsorbed at time t.

Lagergren's first-order kinetic model was also studied to understand the adsorption of methylene blue on CNCs adsorbent. In this model, the assumption is that the rate of solute uptake is proportional to the difference between the amount adsorbed at equilibrium and the adsorbed as a function of time. Various studies have tried this model [21, 22, 23, 24]. Lagergren's first-order model is written as equation (7).

$$\frac{dq_t}{dt} = k_1(q_e - q_t) \quad (7)$$

where, q_e (mg.g^{-1}) is the amount adsorbed at equilibrium, and k_1 (min^{-1}) is the equilibrium rate constant of the pseudo-first-order model.

In addition, the pseudo-second-order adsorption kinetics model is used to predict the mechanism that occurs. In this model, the assumption is that the limiting rate of adsorption is chemisorption, in which the adsorption rate depends on the adsorption capacity, not on the concentration of the adsorbate. The pseudo-second-order model is represented by equation (8).

$$\frac{dq_t}{dt} = k_2(q_e - q_t)^2 \quad (8)$$

Similar to the pseudo-first-order model, k_2 ($g.mg^{-1}.min^{-1}$) implements the equilibrium rate constant of the pseudo-second-order model. The intraparticle diffusion model, which considers the effect of the mass transfer due to diffusion as adsorption resistance, is also used. In simple terms, the model is written as follows:

$$q = k_i\sqrt{t} + C_i \quad (10)$$

where, k_i ($mg.g^{-1}.min^{-1/2}$) and C_i ($mg.g^{-1}$) are the intraparticle diffusion rate and boundary layer thickness indicators, respectively.

The model developed in this research was analogous to the Lagergren first-order model but considered the distribution aspect of the solute in the adsorbent as one of the determining factors. The model is derived from the mass balance as given in equations (11), (12), and (13).

(1) Mass balance of methylene blue in a bulk liquid:

$$\frac{dC_A}{dt} = -\frac{k_c\, a\, m}{V}(C_A - C_A^*) \quad (11)$$

(2) Mass balance of methylene blue in an adsorbent

$$\frac{dX_A}{dt} = k_c a(C_A - C_A^*) \quad (12)$$

(3) Distribution coefficient

$$X_A = K_d C_A^* \quad (13)$$

where, k_c ($m.min^{-1}$), a ($m^2.g^{-1}$), m (g), and V (L) are adsorption rate constants, adsorbent surface area, adsorbent mass, and solution volume, respectively. Meanwhile, C ($mol.L^{-1}$) and C^* ($mol.L^{-1}$) are concentrations over time and concentrations at equilibrium. The concentration of methylene blue on the adsorbent [X_A] ($mol.g^{-1}$) and the adsorption distribution constant [k_D] ($L.g^{-1}$).

3. Results and Discussion

The success of sonication as a support technique in synthesizing CNCs was evaluated using several parameters, including particle size and crystallinity. In short, the effect of sonication is an interesting focus to identify and discuss. Furthermore, CNCs products were used as adsorbents, which have high performance in the adsorption of methylene blue.

3.1. Effect of sonication duration on the degree of crystallinity, crystallite size, and particles size

Information about structure and crystallinity was obtained using XRD. Previous research [25] evaluated various concentrations of NaOH in removing lignin and hemicellulose. XRD diffractograms under selected conditions were referred to in Figure 4a. XRD diffractograms of different sonication durations are shown in Figure 4b. The results of the XRD diffractogram analysis indicate that the CNCs have successfully formed specific crystalline structures and need to be classified. CNCs ranked as cellulose type 1 structures are characterized by the presence of observed peaks at 2θ: 15°, 16.5°, and 23°, which refer to the crystal planes ($1\bar{1}0$), (110), and (200), respectively [26, 27]. The classification of cellulose can also be seen from the two dominant peaks at (110) and (200). The diffraction for the two peaks ranged between 15.5° and 22.5°, indicating a cellulose type 1 structure [28]. However, the observed main peaks are often invisible, which suggests that the isolation of CNCs has to be improved. Nevertheless, the measurement of crystallite size using the Scherrer formula can still be performed, as shown in Table 1.

Table 1. The crystal size of CNCs at various sonication duration based on the Scherrer formula

Duration (min)	2θ (°)	(h k l)	d-spacing (nm)	FWHM	Crystallite size (nm)
15	16.11	(110)	0.49	3.49	2.40
	22.67	(200)	0.39	2.43	3.48
30	15.43	($1\bar{1}0$)	0.57	2.79	3.00
	17.84	(110)	0.50	3.91	2.15
	22.64	(200)	0.39	2.97	2.85
45	15.98	(110)	0.49	3.46	2.42
	22.56	(200)	0.39	3.25	2.60

Crystalline size is an essential parameter in determining the effectiveness of the hydrolysis process. As illustrated in Table 1, the crystal size at (200) tends to decrease with increasing sonication duration. Thus, it can be said that this increase in duration succeeded in reducing the crystalline size of cellulose and successfully forming CNCs.

Additionally, an analysis of crystallinity will provide an essential explanation of the role of sonication itself. The crystallinity of raw material, alkaline, and bleaching were 35.53%, 48.38%, and 50.93%, respectively [29]. Meanwhile, the crystallinity of CNCs for the duration of 15, 30, and 45 min were 61.6%, 55.0%, and 48.4%, respectively. Therefore, this research indicates that increasing time causes a decrease in the crystallinity of CNCs. The possibility of this phenomenon occurs due to the destruction of crystalline cellulose.

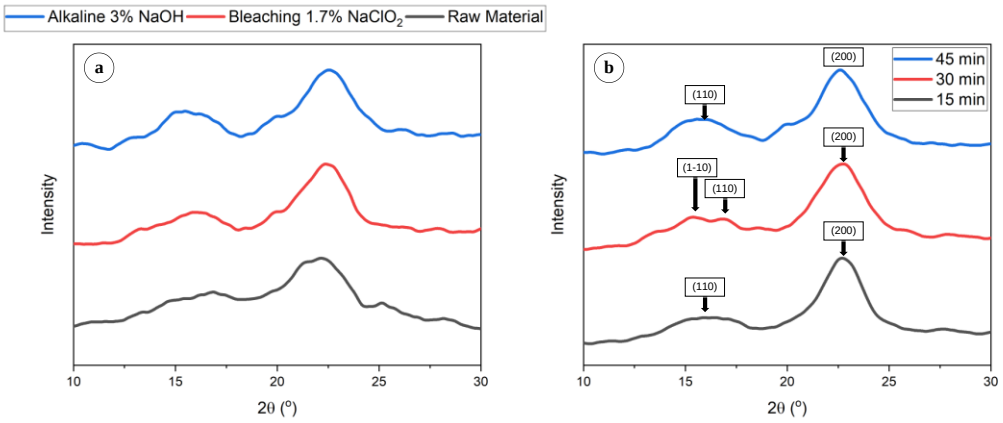

Figure 4. XRD characterization of (a) raw material, bleaching 1.7%$^{(v/v)}$ $NaClO_2$, alkaline 3%$^{(w/w)}$ NaOH (results of previous research [29]), (b) sonication duration of 15, 30, and 45 min

An analogous phenomenon was also found, which reported a decrease in crystallinity of up to 8% with increasing sonication duration. The sonication process was done at a duration of 5, 10, and 15 min with a decrease in crystallinity at 81, 78, and 73%, respectively [30]. The presence of sonication in hydrolysis is indeed essential to assist in the removal of the amorphous region. However, it should also be emphasized that this sonication is nonselective towards the amorphous region and cleaves the crystalline region. Another research by Shojaeiarani *et al.* [31] obtained a similar trend, in which increasing the duration and amplitude of the sonication process resulted in a decrease in the crystallinity of CNCs by up to 12%. Similarly to the present study, crystallinity decreased by 6.58% and 13.22% as sonication time extended (referred values by comparison at 15 min of sonication). The ultrasonic mechanism can be microscopically illustrated in Figure (5).

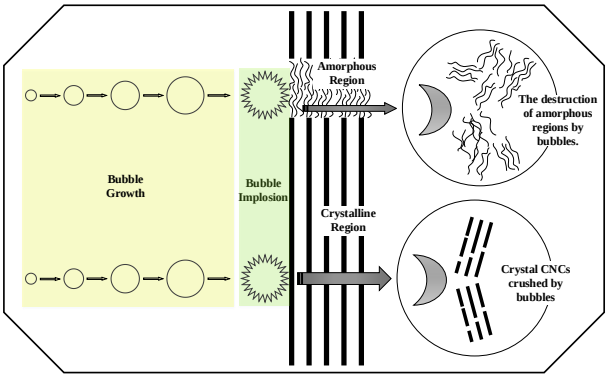

Figure (5). Mechanistic illustration of ultrasonic processes in the production of CNCs

The effectiveness of acid hydrolysis assisted by sonication on the formation of CNCs was also performed by measuring particle size through a particle size analyzer (PSA) in order to confirm that the CNCs were successfully formed. It should be noted that the particle size is the hydrodynamic diameter, which indicates that the CNCs particles are diffused in the solvent. The average hydrodynamic diameter and the average intensity are presented in Table 2.

Table 2. The particle sizes of the prepared CNCs under sonication-assisted hydrolysis based on dynamic light scattering analysis using PSA

Sonication duration (min)	Average hydrodynamic diameter (nm)	Intensity abundance (%)
15	42.35 ± 27.10	75.50 ± 19.94
30	42.99 ± 29.46	80.50 ± 17.71
45	42.63 ± 29.49	78.50 ± 17.23

In the analysis, water is used as a solvent. The water reflection index, viscosity, and fluid temperature are 1.33, 0.8872 cP, and 25°C, respectively. The analysis was repeated four times (quadruplets) to calculate the mean and standard deviation of the particle size of CNCs in water

Based on the data in Table 2, it can be said that the sonication duration has no significant effect on the particle size of CNCs. It also shows that the limitation of particle size reduction is not based on the sonication duration. However, the increasing sonication duration reduced the particle size of the obtained CNCs, with relatively sharp significance [32]. The effect of sonication based on ultrasonic power showed that increasing the power decreased particle size [33]. Although indirectly related to the duration of sonication, sonication affected particle size. There might be a slight difference in the characteristics of the cellulose material and the reagents used in the research. The performance of CNCs as adsorbents also needed to be evaluated in the following section.

3.2. The performance of CNCs as adsorbent for synthetic dye waste

The adsorption performance of CNCs for synthetic dye waste removal was evaluated to determine the relationship between particle size and percent removal and its role in the adsorption rate. The test was done using the steps that had been previously written (section 2). The percent removal of methylene blue is presented in Table 3.

Table 3. Percent removal of methylene blue

Sonication duration (min)	Percent removal (%)
15	73.34
30	73.62
45	72.86

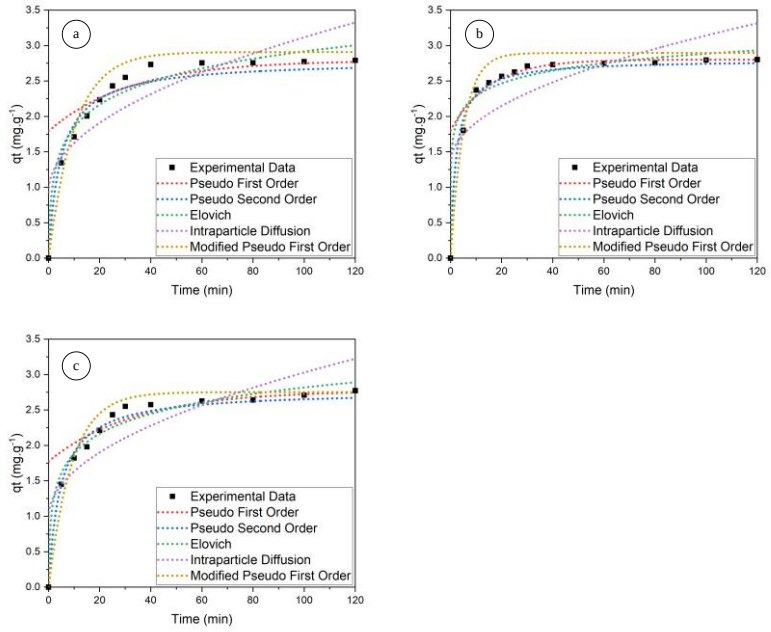

Figure 6. Experimental data and adsorption kinetic models of CNCs at various sonication duration (a) 15, (b) 30, and (c) 45 min

The percent removal in Table 3 confirms that the adsorption performance of methylene blue by CNCs is affected by particle size. Meanwhile, the particle size is correlated with the active surface area of the existing CNCs. Thus, raw materials with nearly identical active surface areas and processes will likely exhibit similar surface properties. As mentioned earlier (section 2), the adsorption mechanism is always related to the surface chemistry of adsorbent material. Many studies related to the adsorption of methylene blue have been reported, some of them using advanced and conventional adsorbents listed in Table 4.

Table 4. Research on the adsorption of methylene blue using various adsorbents

No	Adsorbent	Kinetic model	Removal	Ref.
1	Banana peel–based porous activated carbon	Pseudo-second-order	100%	[34]
2	Dragon fruit peel–based pectin	Pseudo-first-order	35–45%	[35]
3	Dragon fruit peel	Pseudo-second-order	85%	[36]
4	ZnO nanoparticles	-	97%	[37]
5	Cucumber peel	Pseudo-second-order	85%	[38]
6	Iron oxide nanoparticles	Pseudo-second-order	84%	[39]
7	*Phragmites australis*-based biosorbent	Pseudo-second-order	60–72%	[40]
8	*Euchema Spinosum* based biosorbent	Pseudo-second-order	84%	[41]
9	Montmorillonite–graphene oxide composite	Pseudo-second-order	94%	[42]
10	Kaolin–based mesoporous silica	-	>90%	[43]
11	Zeolite–Chitosan composite	Pseudo-second-order	>80%	[44]
12	Halloysite–Cyclodextrin Nanosponges	-	100%	[45]
13	CNCs biosorbent	Pseudo-second-order	±73%	This work

The experimental data and the adsorption kinetic models of various sizes of CNCs are shown in Figure 6. It was found that the adsorption of methylene blue on CNCs was approximated by a pseudo-second-order kinetics model, as evidenced by the highest coefficient of determination (r^2) for each data on various sizes of CNCs. The parameters and correlation coefficients of the various models are detailed in Table 5.

Table 5. Kinetic parameters for adsorption of methylene blue onto CNCs

Models	Parameters	CNCs samples		
		15 min	30 min	45 min
Pseudo-first-order	$q_{e,cal}$	2.769	2.802	2.745
	$q_{e,exp}$	2.792	2.752	2.773
	k_1	0.032±0.021	0.0665±0.045	0.030±0.019
	r^2	0.499	0.520	0.490
Pseudo-second-order	$q_{e,cal}$	2.684	2.753	2.671
	$q_{e,exp}$	2.792	2.752	2.773
	k_2	0.075±0.008	0.166± 0.013	0.078±0.005
	r^2	0.973	0.992	0.988
Elovich	α	2.348±1.136	173.639±258.158	4.150±2.109
	β	2.131±0.245	3.851±0.638	2.459±0.256
	r^2	0.967	0.974	0.976
Intraparticle diffusion	k_P	0.218±0.041	0.180±0.052	0.204±0.041
	C	0.934±0.267	1.345±0.336	0.989±0.265
	r^2	0.737	0.546	0.715
Modified Pseudo-first-order	K_D	26.020	25.554	22.554
	k_C	0.395	0.795	0.427
	r^2	0.982	0.979	0.981

*In the fitting model, two software are used: Origin® 2019b and MATLAB® R2021a. The calculation of the four established models uses a nonlinear curve fit with the Levenberg Marquardt algorithm embedded in the Origin® 2019b. Meanwhile, the modified pseudo-first-order model calculation uses the lsqnonlin and ode15s toolboxes embedded in the MATLAB® R2021a.

Based on Table 5, the adsorption mechanism that occurs is disproportionate to the amount adsorbed, which means that the pseudo-first-order model is unsuitable. This is confirmed by a low coefficient of determination (0.499-0.520). In addition, the adsorption rate of the pseudo-first-order model tends to be linear, in contrast to the actual experimental conditions. The intraparticle diffusion model is also limited in describing the adsorption mechanism of methylene blue by CNCs adsorbents, as evidenced by the low coefficient of determination (0.546-0.737). It demonstrates theoretically that the adsorption resistance due to the diffusion rate of methylene blue onto the adsorbent surface is insignificant.

In contrast, Elovich and pseudo-second-order kinetic models with a chemisorption mechanism approach are likely to correspond with experimental results. However, the pseudo-second-order kinetic model is superior in explaining the mechanism that occurs during adsorption. This is shown at the end of the adsorption model trend tends to be similar to the experimental results, in contrast to the Elovich model does not show a constant adsorption rate at the end of the process. The last approach model (modified pseudo-first-order) provides a strong relationship between the rate of methylene blue being adsorbed and the distribution of the adsorbent. Meanwhile, this model allows the presence of adsorbed methylene blue and its distribution on the adsorbent to play a role in adsorption resistance. Hopefully, this model would implement more real conditions in the experiment. However, the fitting of the developed model has not reached expectations, as the coefficient of determination remains below the pseudo-second-order level. The comparison of the kinetic models of various adsorbents for the adsorption of methylene blue is shown in Table 4. It can be seen that the adsorption tends to conform to the pseudo-second-order model.

4. Conclusion

In this research, the fabrication of CNCs from oil palm trunks as a sustainable adsorbent has been successfully conducted. The results showed that sonication duration affected the crystallinity of CNCs, with a tendency for crystallinity to decrease with increasing sonication duration. However, the particle size of CNCs was unaffected by the sonication duration, and their performance tended to be the same. The pseudo-second-order adsorption kinetics model could approximate the experimental data, showing that the adsorption process was controlled by chemisorption. The best results were obtained from the 15-minute sonication stage.

Acknowledgment

This research was funded by Universitas Gadjah Mada through a research grant of "*Rekognisi Tugas Akhir 2020*" (Contract No. 2488/UN1.P.III/DIT-LIT/PT/2020).

References

[1] Philippe Tingaut, Tanja Zimmermann, Gilles Sèbe, Cellulose nanocrystals and microfibrillated cellulose as building blocks for the design of hierarchical functional materials, *Journal of Materials Chemistry*, 22, 38, (2012), 20105-20111 https://doi.org/10.1039/C2JM32956E

[2] Farshad Hemmati, Seid Mahdi Jafari, Ramezan Ali Taheri, Optimization of homogenization-sonication technique for the production of cellulose nanocrystals from cotton linter, *International Journal of Biological Macromolecules*, 137, (2019), 374-381 https://doi.org/10.1016/j.ijbiomac.2019.06.241

[3] Nathalie Lavoine, Isabelle Desloges, Alain Dufresne, Julien Bras, Microfibrillated cellulose–Its barrier properties and applications in cellulosic materials: A review, *Carbohydrate Polymers*, 90, 2, (2012), 735-764 https://doi.org/10.1016/j.carbpol.2012.05.026

[4] Oleksandr Nechyporchuk, Mohamed Naceur Belgacem, Julien Bras, Production of cellulose nanofibrils: A review of recent advances, *Industrial Crops and Products*, 93, (2016), 2-25 https://doi.org/10.1016/j.indcrop.2016.02.016

[5] Ashvinder Kumar Rana, Elisabete Frollini, Vijay Kumar Thakur, Cellulose nanocrystals: Pretreatments, preparation strategies, and surface functionalization, *International Journal of Biological Macromolecules*, 182, (2021), 1554-1581 https://doi.org/10.1016/j.ijbiomac.2021.05.119

[6] Dileswar Pradhan, Amit K. Jaiswal, Swarna Jaiswal, Emerging technologies for the production of nanocellulose from lignocellulosic biomass, *Carbohydrate Polymers*, 285, 119258, (2022), https://doi.org/10.1016/j.carbpol.2022.119258

[7] Djalal Trache, Vijay Kumar Thakur, Rabah Boukherroub, Cellulose nanocrystals/graphene hybrids—a promising new class of materials for advanced applications, *Nanomaterials*, 10, 8, (2020), 1523 https://doi.org/10.3390/nano10081523

[8] C. N. C. Hitam, A. A. Jalil, Recent advances on nanocellulose biomaterials for environmental health photoremediation: An overview, *Environmental Research*, 204, 111964, (2022), https://doi.org/10.1016/j.envres.2021.111964

[9] Patchiya Phanthong, Guoqing Guan, Yufei Ma, Xiaogang Hao, Abuliti Abudula, Effect of ball milling on the production of nanocellulose using mild acid hydrolysis method, *Journal of the Taiwan Institute of Chemical Engineers*, 60, (2016), 617-622 https://doi.org/10.1016/j.jtice.2015.11.001

[10] Djalal Trache, André Donnot, Kamel Khimeche, Riad Benelmir, Nicolas Brosse, Physico-chemical properties and thermal stability of microcrystalline cellulose isolated from Alfa fibres, *Carbohydrate Polymers*, 104, (2014), 223-230 https://doi.org/10.1016/j.carbpol.2014.01.058

[11] Chinmay Zinge, Balasubramanian Kandasubramanian, Nanocellulose based biodegradable polymers, *European Polymer Journal*, 133, 109758, (2020), https://doi.org/10.1016/j.eurpolymj.2020.109758

[12] Ahmed Fouzi Tarchoun, Djalal Trache, Thomas M. Klapötke, Salim Chelouche, Mehdi Derradji, Wissam Bessa, Abderrahmane Mezroua, A promising energetic polymer from *Posidonia oceanica* brown algae: synthesis, characterization, and kinetic modeling, *Macromolecular Chemistry and Physics*, 220, 22, (2019), 1900358 https://doi.org/10.1002/macp.201900358

[13] Hongjie Dai, Jihong Wu, Huan Zhang, Yuan Chen, Liang Ma, Huihua Huang, Yue Huang, Yuhao Zhang, Recent advances on cellulose nanocrystals for Pickering emulsions: Development and challenge, *Trends in Food Science & Technology*, 102, (2020), 16-29 https://doi.org/10.1016/j.tifs.2020.05.016

[14] Hongxiang Xie, Haishun Du, Xianghao Yang, Chuanling Si, Recent strategies in preparation of cellulose nanocrystals and cellulose nanofibrils derived from raw cellulose materials, *International Journal of Polymer Science*, 2018, 7923068, (2018), https://doi.org/10.1155/2018/7923068

[15] Mohammad Tajul Islam, Mohammad Mahbubul Alam, Alessia Patrucco, Alessio Montarsolo, Marina Zoccola, Preparation of nanocellulose: A review, *AATCC Journal of Research*, 1, 5, (2014), 17-23 https://doi.org/10.14504/ajr.1.5.3

[16] Kok Bing Tan, Alavy Kifait Reza, Ahmad Zuhairi Abdullah, Bahman Amini Horri, Babak Salamatinia, Development of self-assembled nanocrystalline cellulose as a promising practical adsorbent for methylene blue removal, *Carbohydrate Polymers*, 199, (2018), 92-101 https://doi.org/10.1016/j.carbpol.2018.07.006

[17] A. Villabona-Ortíz, C. N. Tejada-Tovar, R. Ortega-Toro, Modelling of the adsorption kinetics of Chromium (VI) using waste biomaterials, *Revista Mexicana de Ingeniería Química*, 19, 1, (2020), 401-408 https://doi.org/10.24275/rmiq/IA650

[18] Jaime López-Luna, Loida E. Ramírez-Montes, Sergio Martinez-Vargas, Arturo I. Martínez, Oscar F. Mijangos-Ricardez, María del Carmen A. González-Chávez, Rogelio Carrillo-González, Fernando A. Solís-Domínguez, María del Carmen Cuevas-Díaz, Virgilio Vázquez-Hipólito, Linear and nonlinear kinetic and isotherm adsorption models for arsenic removal by manganese ferrite nanoparticles, *SN Applied Sciences*, 1, 8, (2019), 1-19 https://doi.org/10.1007/s42452-019-0977-3

[19] Bianca Silva Marques, Tuanny Santos Frantz, Tito Roberto Sant'Anna Cadaval Junior, Luiz Antonio de Almeida Pinto, Guilherme Luiz Dotto, Adsorption of a textile dye onto piaçava fibers: kinetic, equilibrium, thermodynamics, and application in simulated effluents, *Environmental Science and Pollution Research*, 26, 28, (2019), 28584-28592 https://doi.org/10.1007/s11356-018-3587-5

[20] Y. H. Magdy, Hossam Altaher, Kinetic analysis of the adsorption of dyes from high strength wastewater on cement kiln dust, *Journal of Environmental Chemical Engineering*, 6, 1, (2018), 834-841 https://doi.org/10.1016/j.jece.2018.01.009

[21] James Hockaday, Adam Harvey, Sharon Velasquez-Orta, A comparative analysis of the adsorption kinetics of Cu^{2+} and Cd^{2+} by the microalgae *Chlorella vulgaris* and *Scenedesmus obliquus*, *Algal Research*, 64, (2022), 102710 https://doi.org/10.1016/j.algal.2022.102710

[22] Himanshu Gupta, Santosh Singh, Kinetics and thermodynamics of phenanthrene adsorption from water on orange rind activated carbon, *Environmental Technology & Innovation*, 10, (2018), 208-214 https://doi.org/10.1016/j.eti.2018.03.001

[23] Xayanto Inthapanya, Shaohua Wu, Zhenfeng Han, Guangming Zeng, Mengjie Wu, Chunping Yang, Adsorptive removal of anionic dye using calcined oyster shells: isotherms, kinetics, and thermodynamics, *Environmental Science and Pollution Research*, 26, 6, (2019), 5944-5954 https://doi.org/10.1007/s11356-018-3980-0

[24] M. Manjuladevi, R. Anitha, S. Manonmani, Kinetic study on adsorption of Cr(VI), Ni(II), Cd(II) and Pb(II) ions from aqueous solutions using activated carbon prepared from *Cucumis melo* peel, *Applied Water Science*, 8, 1, (2018), 1-8 https://doi.org/10.1007/s13201-018-0674-1

[25] Mega Mustikaningrum, Rochim Bakti Cahyono, Ahmad T. Yuliansyah, Effect of NaOH Concentration in Alkaline Treatment Process for Producing Nano Crystal Cellulose-Based Biosorbent for Methylene Blue, *IOP Conference Series: Materials Science and Engineering*, 2021 https://doi.org/10.1088/1757-899X/1053/1/012005

[26] Wenshuai Chen, Haipeng Yu, Yixing Liu, Peng Chen, Mingxin Zhang, Yunfei Hai, Individualization of cellulose nanofibers from wood using high-intensity ultrasonication combined with chemical pretreatments, *Carbohydrate Polymers*, 83, 4, (2011), 1804-1811 https://doi.org/10.1016/j.carbpol.2010.10.040

[27] Juan Guo, Xuxia Guo, Siqun Wang, Yafang Yin, Effects of ultrasonic treatment during acid hydrolysis on the yield, particle size and structure of cellulose nanocrystals, *Carbohydrate Polymers*, 135, (2016), 248-255 https://doi.org/10.1016/j.carbpol.2015.08.068

[28] Peng Tao, Yuehua Zhang, Zhengmei Wu, Xiaoping Liao, Shuangxi Nie, Enzymatic pretreatment for cellulose nanofibrils isolation from bagasse pulp: transition of cellulose crystal structure, *Carbohydrate Polymers*, 214, (2019), 1-7 https://doi.org/10.1016/j.carbpol.2019.03.012

[29] Fahmi Fathurrahman Miranda, Aristawati Sekar Putri, Mega Mustikaningrum, Ahmad Tawfiequrrahman Yuliansyah, Preparation and characterization of nano crystal cellulose from oil palm trunk for adsorption of methylene blue, *AIP Conference Proceedings*, 2021 https://doi.org/10.1063/5.0067128

[30] Wei Li, Jinquan Yue, Shouxin Liu, Preparation of nanocrystalline cellulose via ultrasound and its reinforcement capability for poly (vinyl alcohol) composites, *Ultrasonics Sonochemistry*, 19, 3, (2012), 479-485 https://doi.org/10.1016/j.ultsonch.2011.11.007

[31] Jamileh Shojaeiarani, Dilpreet Bajwa, Greg Holt, Sonication amplitude and processing time influence the cellulose nanocrystals morphology and dispersion, *Nanocomposites*, 6, 1, (2020), 41-46 https://doi.org/10.1080/20550324.2019.1710974

[32] Luana Müller de Souza, Renato Queiroz Assis, Cristian Mauricio Barreto Pinilla, Rafaela Stange, Helena Cristina Vieira, Adriano Brandelli, Tania Maria Haas Costa, Alessandro de Oliveira Rios, Polliana D'Angelo Rios, *Eucalyptus* spp. cellulose nanocrystals obtained by acid hydrolysis and ultrasound processing for structural strengthening in paper packaging, *Wood Science and Technology*, 55, 3, (2021), 639-657 https://doi.org/10.1007/s00226-021-01278-6

[33] Longwei Jiang, Jingde Yang, Qian Wang, Lili Ren, Jiang Zhou, Fabrication and characterisation of cellulose nanocrystals from microcrystalline cellulose by esterification and ultrasound treatment, *Micro & Nano Letters*, 13, 11, (2018), 1574-1579 https://doi.org/10.1049/mnl.2018.5043

[34] Yan Lu, Sizhong Li, Preparation of hierarchically interconnected porous banana peel activated carbon for methylene blue adsorption, *Journal of Wuhan University of Technology-Mater. Sci. Ed.*, 34, 2, (2019), 472-480 https://doi.org/10.1007/s11595-019-2076-0

[35] M. F. Abdullah, Ahmad Azfaralariff, Azwan Mat Lazim, Methylene blue removal by using pectin-based hydrogels extracted from dragon fruit peel waste using gamma and microwave radiation polymerization techniques, *Journal of Biomaterials Science, Polymer Edition*, 29, 14, (2018), 1745-1763 https://doi.org/10.1080/09205063.2018.1489023

[36] Ali H. Jawad, Afaf Murtadha Kadhum, Y. S. Ngoh, Applicability of dragon fruit (*Hylocereus polyrhizus*) peels as low-cost biosorbent for adsorption of methylene blue from aqueous solution: kinetics, equilibrium and thermodynamics studies, *Desalination and Water Treatment*, 109, (2018), 231-240 http://dx.doi.org/10.5004/dwt.2018.21976

[37] C. A. Soto-Robles, O. J. Nava, A. R. Vilchis-Nestor, A. Castro-Beltrán, C. M. Gómez-Gutiérrez, E. Lugo-Medina, A. Olivas, P. A. Luque, Biosynthesized zinc oxide using *Lycopersicon esculentum* peel extract for methylene blue degradation, *Journal of Materials Science: Materials in Electronics*, 29, 5, (2018), 3722-3729 https://doi.org/10.1007/s10854-017-8305-4

[38] Sadia Shakoor, Abu Nasar, Adsorptive treatment of hazardous methylene blue dye from artificially contaminated water using *cucumis sativus* peel waste as a low-cost adsorbent, *Groundwater for Sustainable Development*, 5, (2017), 152-159 https://doi.org/10.1016/j.gsd.2017.06.005

[39] Alireza Allafchian, Zahra Sadat Mousavi, Seyed Sajjad Hosseini, Application of cress seed musilage magnetic nanocomposites for removal of methylene blue dye from water, *International Journal of Biological Macromolecules*, 136, (2019), 199-208 https://doi.org/10.1016/j.ijbiomac.2019.06.083

[40] Rania Dallel, Aida Kesraoui, Mongi Seffen, Biosorption of cationic dye onto "*Phragmites australis*" fibers: Characterization and mechanism, *Journal of Environmental Chemical Engineering*, 6, 6, (2018), 7247-7256 https://doi.org/10.1016/j.jece.2018.10.024

[41] Nadiah Mokhtar, Edriyana A. Aziz, Azmi Aris, W. F. W. Ishak, Noor Saadiah Mohd Ali, Biosorption of azo-dye using marine macro-alga of *Euchema Spinosum*, *Journal of Environmental Chemical Engineering*, 5, 6, (2017), 5721-5731 https://doi.org/10.1016/j.jece.2017.10.043

[42] Yang Yang, Weiye Yu, Shujun He, Shuaixian Yu, Ying Chen, Luhua Lu, Zhu Shu, Hongda Cui, Yong Zhang, Hongyun Jin, Rapid adsorption of cationic dye-methylene blue on the modified montmorillonite/graphene oxide composites, *Applied Clay Science*, 168, (2019), 304-311 https://doi.org/10.1016/j.clay.2018.11.013

[43] Tiantian Li, Zhu Shu, Jun Zhou, Yun Chen, Dongxue Yu, Ximing Yuan, Yanxin Wang, Template-free synthesis of kaolin-based mesoporous silica with improved specific surface area by a novel approach, *Applied Clay Science*, 107, (2015), 182-187 https://doi.org/10.1016/j.clay.2015.01.022

[44] W. A. Khanday, M. Asif, B. H. Hameed, Cross-linked beads of activated oil palm ash zeolite/chitosan composite as a bio-adsorbent for the removal of methylene blue and acid blue 29 dyes, *International Journal of Biological Macromolecules*, 95, (2017), 895-902 https://doi.org/10.1016/j.ijbiomac.2016.10.075

[45] Marina Massaro, Carmelo G. Colletti, Giuseppe Lazzara, Susanna Guernelli, Renato Noto, Serena Riela, Synthesis and characterization of halloysite–cyclodextrin nanosponges for enhanced dyes adsorption, *ACS Sustainable Chemistry & Engineering*, 5, 4, (2017), 3346-3352 https://doi.org/10.1021/acssuschemeng.6b03191